Available online at www.sciencedirect.com

SCIENCE DIRECT®

Journal of Photochemistry and Photobiology A: Chemistry 162 (2004) 563–567

Journal of Photochemistry and Photobiology A:Chemistry

www.elsevier.com/locate/jphotochem

Photochemistry of group IV porphyrin halides

Bradford J. Pistorio, Daniel G. Nocera*

Department of Chemistry, Massachusetts Institute of Technology, 6-335, 77 Massachusetts Ave., Cambridge, MA 02139-4307, USA

Received 7 August 2003; received in revised form 30 September 2003; accepted 1 October 2003

Abstract

The photochemistry of early transition metal porphyrins (TPP)ZrX_2 and (TTP)TiCl (TPP = tetraphenylporphyrin, TTP = tetratolylporphyrin, X = Br, Cl) was investigated. Chemical reduction and electrochemical studies indicated that the porphyrin macrocycle is more easily reduced than the metal centers. The same trend is observed under photochemical conditions of UV and near-UV excitation, where photoreduction of the porphyrin macrocycle is observed, as opposed to M–X photoelimination.

Keywords: Porphyrins; Photochemistry; Dihalides; Hydrogen; Energy conversion; Titanium; Zirconium

1. Introduction

The photoproduction of hydrogen from acidic solutions is a fundamental transformation of many energy conversion cycles. The H_2 photocatalytic cycle shown in Scheme 1 is based on the oxidative-addition of HX to a metal center to produce a metal–hydrido halo complex, which subsequently reacts with an additional equivalent of HX to produce H_2 and the metal dihalide. Photoactivation of the M–X bond and elimination of X_2 regenerates the original metal complex to complete the cycle; this latter reaction is the primary obstacle to establishing the photocycle. Indeed, metal complexes commonly react with HX to produce H_2 and the metal dihalide. The M–X bond, however, is thermodynamically robust and kinetically inert. A focus of recent efforts has been to exploit the two-electron mixed-valency of bimetallic centers of late transition metals (M = Rh, Ir) [1–3] to overcome the impediment posed by M–X bonds [1,4]. We have shown that the Rh^{II}–X bonds of a $Rh^0Rh^{II}X_2$ core may be photoactivated to yield a LRh^0–Rh^0 catalyst, which subsequently reacts with HX to produce hydrogen [5]. A photocatalytic cycle may therefore be established according to Scheme 1.

We are interested in exploring the generality of Scheme 1 by exploring the M–X photochemistry of other classes of metal complexes [6]. In the work described here, we test the limits of early transition metalloporphyrins as candidates for effecting the photocycle in Scheme 1. We were attracted to metalloporphyrins for H_2 photocatalysis for several reasons. Firstly, early transition metal porphyrins prefer a *cis*-halide arrangement; the proximity of the halides is conducive to X–X coupling. Secondly, metalloporphyrin systems may be expected to react facilely with HX to produce hydrogen. Along these lines, *cis*-dimethyl(*meso*-tetraphenylporphyrinato) zirconium(IV) [(TPP)$ZrMe_2$] has been shown to eliminate ethane upon irradiation with visible light ($\lambda_{exc} > 420$ nm) [7]. Moreover, [$Cp_2Zr(H)Cl$] or [$Cp^*_2Zr(H)Cl$] are expected to display surrogate reactivity to that of group IV metalloporphyrins. Treatment of these Zr(IV) hydrido–halo compounds with HX yields H_2 [8,9]. On this basis, early transition metalloporphyrins may be expected to support the chemistry of Scheme 1 by cleanly reacting with HX to produce H_2 and metal dihalide. Notwithstanding, we show here that the M–X bonds of early transition metalloporphyrins are too strong to support the photocycle of Scheme 1. Instead, photoexcitation of *cis*-dihalide metalloporphyrins results in photoreduction of the porphyrin macrocycle, thereby circumventing M–X photoactivation.

2. Experimental

2.1. Materials and syntheses

All synthetic manipulations were conducted in a dry and oxygen-free environment provided by either a Schlenk-line or N_2 glove box unless otherwise noted. Solvents for synthesis were reagent grade and were dried by following standard procedures: tetrahydrofuran, diethyl ether, hexanes, benzene, and pentane were all distilled from sodium/benzophenone; toluene was distilled from sodium; and dichloromethane

---

* Corresponding author. Tel.: +1-617-253-5537; fax: +1-617-253-7670.
E-mail address: nocera@mit.edu (D.G. Nocera).

1010-6030/$ – see front matter © 2004 Elsevier B.V. All rights reserved.
doi:10.1016/S1010-6030(03)00399-X

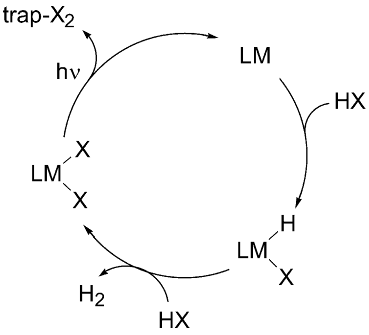

Scheme 1.

was distilled from calcium hydride under N_2 [10]. Toluene was kept over 4 Å molecular sieves to ensure dryness. All NMR solvents were dried over calcium hydride, purified by distillation and stored over 4 Å molecular sieves. Elemental analyses were performed at H. Kolbe Mikroanalytisches Laboratorium. Silica gel 60 (70–230 and 230–400 mesh, Merck) was used for chromatography. The starting materials were used as received: sodium acetate, pyridine, benzonitrile, $Li[N(SiMe_3)_2]$, SiX_4 and ZrX_4 (X = Cl, Br) were purchased from Sigma–Aldrich. Tetraphenylporphyrin was prepared by published procedures, while metallated porphyrins were prepared by adaptation of literature procedures [11–18]. $ZrX_4(THF)_2$ (X = Cl, Br) was prepared by addition of a stoichiometric amount of THF to $ZrCl_4$ in CH_2Cl_2 followed by precipitation with hexane [19]. $(TPP)Li_2(THF)_2$ [17,21], $(TTP)Li_2(THF)_2$ [20], $(TPP)ZrCl_2$ [11–16,21] and $(TPP)Zr(OAc)_2$ [22] were prepared according to previously published procedures. These materials gave satisfactory ^1H NMR spectra and mass spectral analysis.

2.1.1. *(TPP)ZrBr$_2$*

The dibromide was prepared according to two methods developed for the chloride companion compound: from the lithiated porphyrin [17,21] and from diacetate [22]. $ZrBr_4(THF)_2$ (0.410 g, 0.532 mmol) and $(TPP)Li_2(THF)_2$ (0.298 g, 0.538 mmol) were dissolved in dry toluene (150 ml) under an inert atmosphere and refluxed for about 6–12 h in a 1 L Schlenk flask. The toluene was then removed and the resulting brick red product was collected and recrystallized from toluene/hexane solutions to give a brilliant red solid (0.252 g, 55% yield). ^1H NMR (300 MHz, C_6D_6): 8.99 (s, 8H, pyrrole-β), 8.15, 7.80 (dd, 8H, *o*-Ph-), 7.41 (m, 12H, *m*,*p*-Ph-). UV-Vis (CH_2Cl_2, λ_{max}, nm): 399, 418 (Soret), 512, 540. Anal. found (calcd.) for $C_{44}H_{28}Br_2N_4Zr$: C 61.23 (61.18), H 3.65 (3.27), N 6.45 (6.49) Br 18.89 (18.50).

Alternatively, the lithiated porphyrin precursor may be bypassed if the dibromide complex is prepared from $(TPP)Zr(OAc)_2$. $(TPP)Zr(OAc)_2$ (0.108 g, 0.131 mmol) was added to toluene (50 ml) contained within a 100 ml Schlenk flask equipped with a reflux condenser. Upon addition of trimethylsilyl bromide (60 μl, 0.455 mmol), the solution changed from a light red to a deep red color. The solution was heated for 3 h, after which the toluene was evaporated to about 5 ml. Hexane (15 ml) was added to precipitate the red product that was recrystallized to give (TPP)Zr(OAc)Br (0.105 g) in 95% yield. ^1H NMR (300 MHz, $CDCl_3$): 9.09 (s, 8H, pyrrole-β), 8.38, 8.13 (br dd, 8H, *o*-Ph-), 7.84 (m, 12H, *m*,*p*-Ph-), 0.27 (s, 3H, -O_2CCH_3). UV-Vis (CH_2Cl_2, λ_{max}, nm): 399, 418 (Soret), 540. IR (KBr) $\nu(OCOCH_3)$: 1470 cm^{-1}. Anal. found (calcd.) for $C_{46}H_{31}BrN_4O_2Zr$: C 64.47 (65.55), H 3.70 (3.74), N 6.45 (6.65). The (TPP)Zr(OAc)Br (0.050 g, 0.594 mmol) and 2 equiv of $ZrBr_4$ (0.050 g, 0.122 mmol) were refluxed for 18 h in toluene (25 ml). The solvent was then reduced to 10 ml and the remaining solution was filtered through a filter pipette containing about 3 cm of SiO_2. The filtered solution was evaporated and the remaining solid was recrystallized from a toluene/hexane solvent system to afford $(TPP)ZrBr_2$ in 81% yield (0.042 g). The ^1H NMR and UV-Vis spectral data were identical those observed for product afforded from the foregoing synthetic procedure.

2.1.2. *Reduction of (TPP)ZrX$_2$ complexes*

A 1 cm^3 quartz cell of a high vacuum apparatus was charged with a ca. 10^{-5} M THF solution of $(TPP)Zr(OAc)_2$ (500 μl). The THF was evacuated to dryness and brought into the glove box. A small drop of 0.5% Na–Hg amalgam and 5 ml of dry THF were placed in the solvent reservoir of the apparatus. The cell was removed from the dry box. About 2 ml of the THF and the 0.5% Na–Hg amalgam were introduced to the cell containing the porphyrin. The solution was vigorously shaken and the color changed from red to bright green. The UV-Vis spectrum indicated of the reduced product is (λ_{max}, nm): 453 (Soret), 650, 800.

A ca. 10^{-5} M THF solution (500 μl) of $(TPP)ZrX_2$ (X = Cl, Br) was introduced to a 1 cm^3 quartz cell of a high vacuum apparatus. The THF was evacuated to dryness and brought into the glove box. The solvent reservoir was charged with a small drop of 0.5% Na–Hg amalgam and 5 ml of dry THF. The cell was removed from the dry box. About 2 ml of the THF and the 0.5% Na–Hg amalgam were introduced to the cell containing the porphyrin. The solution changed from red to bright green upon vigorous shaking. For X = Cl: UV-Vis (λ_{max}, nm): 453 (Soret), 650, 800. EPR (298 K, toluene): $g = 2.0049$. For X = Br: UV-Vis (λ_{max}, nm): 453 (Soret), 560, 805.

2.1.3. *(TTP)TiCl*

The complex was prepared by following a derivative route for obtaining the TPP analog [18]. A Schlenk flask was equipped with a stir bar, a Vigreux column and a N_2 inlet adapter and charged with $(TTP)Li(THF)_2$ (0.256 g, 0.310 mmol) and $TiCl_3(THF)_2$ (0.124 g, 0.335 mmol) in toluene (15 ml). The solution was gently heated at 60 °C for about 7 h, in which the color changed slowly from blue–green to purple. The solution was filtered and the solvent was completely removed. A small portion of CH_2Cl_2 was added to redissolve the paste; the solution was layered with pentane and stored in a freezer overnight. The purple crystals were collected and dried (55%). ^{1}H NMR (300 MHz, $CDCl_3$): 2.37 (br s, 12H, –CH_3). UV-Vis (toluene, λ_{max}, nm): 401, 418 (Soret), 512, 552, 593. EI/MS ($C_{48}H_{36}ClN_4Ti$) *m/z*, found (calcd): $[M]^+$ 751 (751), $[M–Cl]^+$ 715 (715).

2.2. Photochemical methods

Stoichiometric photolysis experiments were carried out in high vacuum cells composed of a 1 cm quartz cell (Starna Cells Inc.) with borosilicate grated seal and a 10 ml solvent reservoir isolated from each other and the atmosphere by teflon stopcocks (Kontes). Spectroscopic grade THF (Burdick and Jackson) was refluxed and distilled over Na and freeze–pump–thawed prior to use. The dry THF was added to the cell by vacuum transfer and subjected to additional freeze–pump–thawed cycles (10^{-6} Torr). Bulk photolysis experiments were performed in 100 ml custom Pyrex tubes with quartz window seal with a diameter of about 10 cm. Samples were irradiated with light from a 1000-W high pressure Oriel Hg–Xe lamp. The two-inch collimated light beam passed through a water filter to remove infrared wavelengths and long wave pass filters to remove high-energy light prior to focusing and collimating to a diameter of about 0.5 in. The high-energy cut-off filters were replaced with 10 nm band pass mercury line interference filters (Oriel) for quantum yields measured using the standard ferrioxalate actinometer just before and just after sample irradiation. The progress of the photoreaction was monitored by UV-Vis spectra, which were recorded on a Spectral Instruments model 440 with integrating CCD array detector and fiber optic sampler and the UV-Vis samples were recorded in quartz cells isolated from air by teflon stopcocks.

2.3. Physical methods

All NMR spectra were collected at the MIT Department of Chemistry Instrumentation Facility (DCIF) on a Varian Inova Unity 300 or Varian Mercury 300 spectrometer at 293 K. NMR solvents C_6D_6 and $CDCl_3$ (Cambridge Isotope Laboratories) were dried using appropriate agents and degassed by at least three freeze–pump–thaw cycles. NMR samples were contained in Teflon sealed NMR tubes free of O_2. All chemical shifts are reported using the standard δ notation in parts-per-million; positive chemical shifts are to a higher frequency from the given reference. X-band EPR spectra were recorded in toluene at 298 K in 4 mm quartz tubes on a Bruker 300 EMX EPR spectrometer, using the Win-EPR program. UV-Vis spectra were recorded on a Spectral Instruments model 440 with integrating CCD array detector and fiber optic sampler. All UV-Vis samples were recorded in quartz cells isolated from air. Electron ionization (EI) and thermospray ionization (ESI) mass spectral analyses were performed at the MIT DCIF. IR spectra were recorded on a Nicolet Impact 410 spectrometer.

Cyclic voltammetric measurements were carried out with a BAS 100 electrochemical analyzer. A three-electrode system comprised a glassy carbon ($A = 0.08\,cm^2$), a Pt-wire and a Ag/AgCl wire working, counter and reference electrodes, respectively. A 0.1 M solution of $(TBA)PF_6$ in freshly distilled CH_2Cl_2 was used as a supporting electrolyte during the electrochemical experiments. All solutions were degassed with Ar for 20 min prior to measurement and blanketed with Ar during the course of the electrochemical experiments. The scan rate was 50 mV/s and the scan range was 5–1500 mV. Cyclic voltammetric waves were referenced to a $[Cp_2Fe]^{+/0}$ couple.

3. Results and discussion

$(TPP)ZrX_2$ complexes were prepared by the methods shown in Scheme 2. The dihalides may be obtained by refluxing lithiated porphyrins $(TPP)Li_2(THF)_2$ with the bis(tetrahydrofuran) metal halide compound, $ZrX_4(THF)_2$ [11–16]. The lithiated precursors are made in high yield

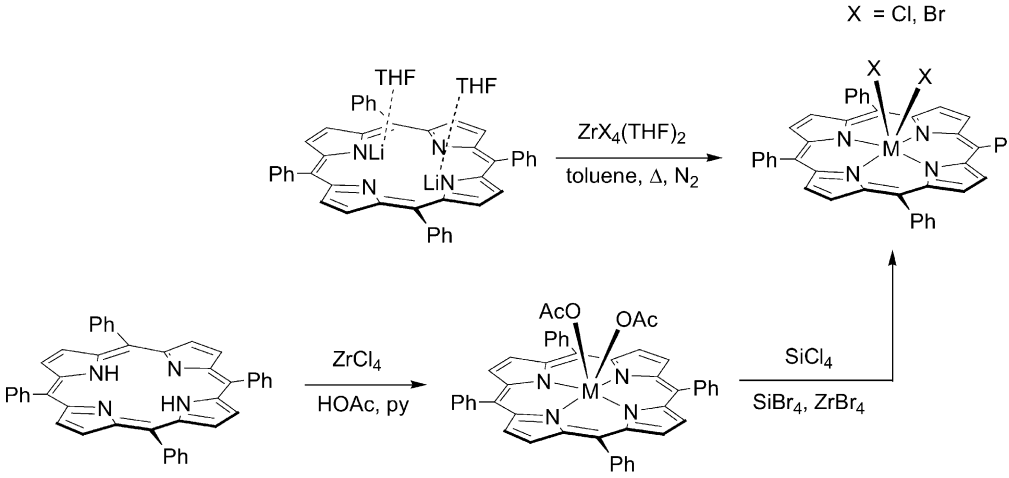

Scheme 2.

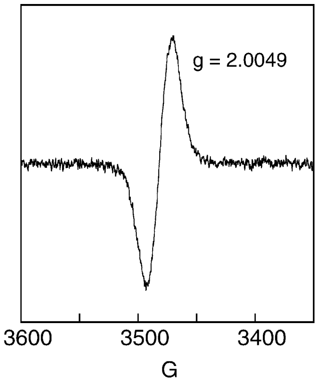

Fig. 1. The EPR spectrum obtained upon the Na–Hg reduction of $(TPP)ZrCl_2$ in toluene at 298 K.

by reacting an excess of lithium bis(trimethylsilyl)amide $Li[N(SiMe_3)_2]$ with free-base porphyrin in boiling THF under N_2 [17]. Alternatively, $(TPP)Zr(OAc)_2$ affords product in high yield without the need for the lithiated porphyrins or air-sensitive compounds [21–23]. Satisfactory mass spectral data and elemental analyses were obtained for $(TPP)ZrX_2$ and $(TPP)Zr(OAc)_2$ complexes.

The reduction of $(TPP)ZrX_2$ (X = Cl, Br) porphyrins was examined by electrochemical and chemical means. Anaerobic THF solutions of the porphyrins readily react with 0.5% Na–Hg at room temperature. Electronic absorption and EPR spectra indicate that the porphyrin macrocycle is more easily reduced than the Zr(IV) center. An absorption band at 800 nm for the reduced porphyrins is characteristic of the π-anion radical [24–26]. The isotropic EPR signal with $g = 2.0049$ for the $(TPP)ZrCl_2$ reduction product (Fig. 1) is also typical of a radical [27,28]. Similar results are obtained for electrochemical reductions. Cyclic voltammograms of CH_2Cl_2 solutions of $(TPP)ZrCl_2$ were measured in 0.1 M *n*-tetrabutylammonium hexafluorophosphate with a scan rate of 50 mV/s at a glassy carbon working electrode ($A = 0.08\,cm^2$). In all cases, a pronounced, quasi-reversible reduction wave at ca. −1.30 V (versus Ag/AgCl) is observed (Table 1). This wave is characteristic of the one-electron reduction of the porphyrin macrocycle [24–26]. These data clearly demonstrate the formation of the porphyrin radical anion, and the inability to reduce the Zr(IV) metal center.

The photochemistry of $(TPP)ZrX_2$ complexes is concordant with electrochemical and chemical reactivity studies. THF solutions of $(TPP)ZrCl_2$ in the presence of 0.2 M 2,6-lutidine are photoinert under visible or UV irradiation conditions. This result indicates that $(TPP)ZrCl_2$ does not undergo the stepwise photoelimination of $Cl^\bullet$ radicals, as they would be immediately trapped by THF [1,4,5]. Moreover $(TPP)ZrCl_2$ is photoinert in the presence of various Cl_2 traps. A sluggish, albeit clean, photoreaction is observed when $(TPP)ZrCl_2$ is irradiated in the presence of PCl_3. The evolution of the absorption profile with photolysis of $(TPP)ZrCl_2$ in a degassed (10^{-6} Torr) 2.0 M PCl_3/benzene solution is shown in Fig. 2. The initial spectrum, which is maintained indefinitely in the absence of light, changes slowly upon irradiation with visible light ($\lambda_{exc} > 530$ nm). Well-anchored isosbestic points maintained throughout the irradiation attest to a clean and quantitative photoreaction. With the appearance of the final absorption spectrum, no additional changes are observed with further irradiation. The final absorption spectrum is similar to that obtained for the chemical reduction of $(TPP)ZrCl_2$. In addition, no PCl_5 was observed in the $^{31}P\{^1H\}$ NMR of bulk photolyzed solutions, indicating that Cl_2 is not photoeliminated from $(TPP)ZrCl_2$ platforms. We believe that the reducing source of the photoreaction is likely polyphosphorus acid, an impurity in PCl_3 solutions under reduced pressures at room temperature. Alternatively, PCl_3 may be the source of photoreduction by a presently undetermined mechanism.

The very strong Zr–X bonds and unfavored $Zr^{4+/3+}$ reduction potential precludes Zr^{IV}–X photoactivation. We therefore turned our attention to titanium analogs, which have weaker metal-halide bonds and an accessible $M^{4+/3+/2+}$ redox couples. Nevertheless, photochemical experiments reveal that the establishment of the photocycle in Scheme 1 is again prevented by the inability to photocleave the Ti–X bond. Unlike the $(TPP)ZrX_2$ system, however, photoactivation of the M–X bond is disfavored from the M^{3+} oxidation state (versus the M^{4+} oxidation state of the zirconium porphyrins). A 0.2 M THF solution of

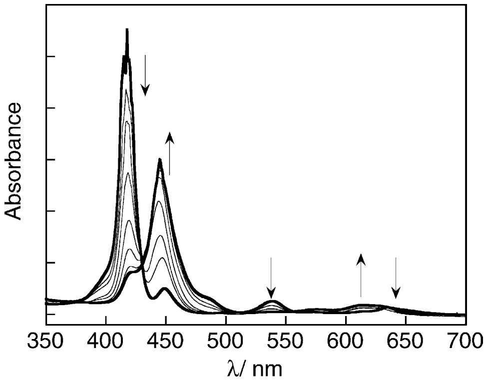

Fig. 2. Changes in the absorption profile during photolysis ($\lambda_{exc} > 530$ nm) of a benzene solution of $(TPP)ZrCl_2$ (ca. 10^{-6} M) in the presence of PCl_3 (ca. 2.0 M) at 293 K. The arrows indicate the disappearance of $(TPP)ZrCl_2$ and the appearance of a reduced zirconium porphyrin photoproduct. Spectra were recorded over the span of 10 days at ∼1-day intervals.

Table 1
UV-Vis[a], EPR[b], and potentials[c] for reduced zirconium(IV) porphyrins

	$\lambda_{abs,max}$ (nm)	*g*-value	$E_{1/2}$ (V)[c]
$(TPP)Zr(OAc)_2$	453, 650 (sh), 800	–	−1.27
$(TPP)ZrBr_2$	453, 560, 805	–	−1.37
$(TPP)ZrCl_2$	453, 650 (sh), 800	2.0049	−1.27

[a] Porphyrin complexes were reduced in THF solution.

[b] Porphyrin complexes were reduced in toluene solution.

[c] Cyclic voltammograms of porphyrins were performed in CH_2Cl_2 containing 0.1 M $(TBA)PF_6$ as supporting electrolyte with a scan rate of 50 mV/s. Potentials are reported vs. the Ag/AgCl reference.

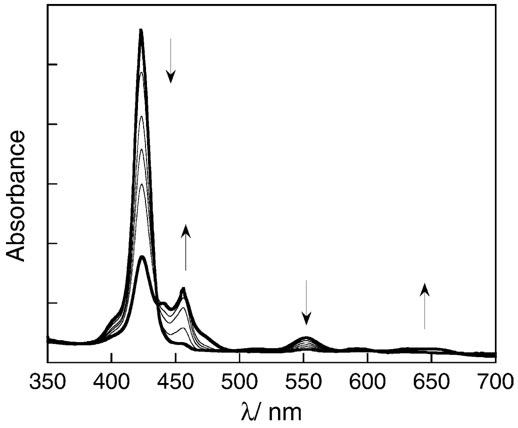

Fig. 3. Absorption profiles of a photolyzed ($\lambda_{exc} > 435$ nm) THF solution of (TTP)TiCl (ca. 10^{-6} M) in the presence of 2,6-lutidine (ca. 0.2 M) at 293 K. The arrows indicate the disappearance of (TTP)TiCl and the appearance of the reduced titanium porphyrin photoproduct. Spectra were recorded over the span of 48 h at ~12-h intervals.

(TTP)TiCl and 2,6-lutidine is photosensitive upon irradiation with $\lambda_{exc} > 435$ nm. As shown in Fig. 3, isosbestic points are maintained throughout the course of the photoreaction; however, the final spectrum does not correspond to the known titanium(II) complex, (TTP)Ti(THF)$_2$. Rather, the spectrum is remarkably similar to that obtained for (TPP)Zr^{IV}Cl$_2$ photolysis (see Fig. 2). This result indicated that photoreduction of the TPP macrocycle is preferred versus Ti^{3+} photoreduction.

In summary, the metal–halogen bond strengths of early transition metalloporphyrins are too strong to be broken with near UV or visible light. The redox potentials for early transition metal complexes as compared to the porphyrin ring are such that reduction proceeds at the latter cofactor as opposed to Zr^{4+} and Ti^{3+} metal centers of (TPP)MX$_2$ and (TTP)MX complexes, respectively. These results clearly establish that H$_2$ producing photocycles relying on M–X photoactivation cannot be realized with early transition metalloporphyrins. Accordingly, later transition metal porphyrin complexes pose a more promising avenue for metal–halogen photoactivation toward hydrohalic acid splitting reactivity. The Rh–X bonds of porphyrin platforms may be particularly susceptible to photoactivation. However, such platforms are characterized by a single Rh–X bond. Two porphyrins must therefore be brought together to induce X–X coupling upon Rh–X photoactivation. To this end, our preparation of the Pacman porphyrins anchored to DPX (diporphyrin xanthene) and DPD (diporphyrin dibenzofuran) pillars [29,30] look to be promising platforms for HX photochemistry. The construct confines two porphyrins in a face-to-face geometry. The neighboring porphyrins display an extensive range of vertical pocket size dimensions and flexibilities with minimal lateral displacements between macrocyclic subunits [29–32] and metal-atom bonds within the cofacial cleft of the Pacman porphyrins may be photoactivated [30,33]. For these reasons, the photochemistry of DPX and DPD Rh$_2$X$_2$ Pacman porphyrins appear to be an intriguing line of inquiry.

Acknowledgements

This work was supported by a grant from the National Science Foundation (CHE-0132680).

References

[1] A.F. Heyduk, A.M. Macintosh, D.G. Nocera, J. Am. Chem. Soc. 121 (1999) 5023–5032.
[2] A.F. Heyduk, D.G. Nocera, Chem. Commun. (1999) 1519–1520.
[3] A.F. Heyduk, D.G. Nocera, J. Am. Chem. Soc. 122 (2000) 9415–9426.
[4] A.L. Odom, A.F. Heyduk, D.G. Nocera, Inorg. Chim. Acta 297 (2000) 330–337.
[5] A.F. Heyduk, D.G. Nocera, Science 293 (2001) 1639–1641.
[6] B.J. Pistorio, D.G. Nocera, Chem. Commun. (1999) 1831–1832.
[7] K. Shibata, T. Aida, S. Inoue, Chem. Lett. (1992) 1171–1176.
[8] P.C. Wailes, H. Weigold, J. Organomet. Chem. 2 (1970) 405–411.
[9] B.J. Pistorio, D.G. Nocera, unpublished results.
[10] W.L.F. Amarego, D.D. Perrin, Purification of Laboratory Chemicals, 4th ed., Butterworths–Heinmann, Oxford, 1996.
[11] B.D. Berezin, T.N. Lomova, J. Russ. Inorg. Chem. 26 (1981) 203–207.
[12] H.J. Kim, D. Whang, K. Kim, Y. Do, Inorg. Chem. 32 (1993) 360–362.
[13] J.W. Buchler, Liebigs. Ann. Chem. 745 (1971) 135–151.
[14] J.W. Buchler, A. de Cian, J. Fischer, P. Hammerschmitt, R. Weiss, Chem. Ber. 124 (1991) 1051–1058.
[15] H.J. Kim, S. Jung, Y.M. Jeon, D. Whang, K. Kim, Chem. Commun. (1997) 2201–2202.
[16] J.W. Buchler, M. Eberle, Chem. Ber. 128 (1995) 1131–1133.
[17] J. Arnold, Chem. Commun. (1990) 976–978.
[18] L.M. Berreau, J.A. Hays, V.G. Young Jr., L.K. Woo, Inorg. Chem. 33 (1994) 105–108.
[19] L.E. Manzer, Inorg. Synth. 21 (1982) 135–140.
[20] H. Brand, J.A. Capriotti, J. Arnold, Inorg. Chem. 33 (1994) 4334–4337.
[21] J. Arnold, B. Brand, Organometallics 12 (1993) 3656–3662.
[22] J.L. Huhmann, J.Y. Corey, N.P. Rath, C.F. Campana, J. Organomet. Chem. 513 (1996) 17–26.
[23] K. Shibata, T. Aida, S. Inoue, Tetrahedron Lett. 33 (1992) 1077–1082.
[24] K.M. Kadish, B. Boisselier-Cocolois, P. Cocolois, R. Guilard, Inorg. Chem. 24 (1985) 2139–2147.
[25] K.M. Kadish, B. Boisselier-Cocolois, P. Cocolois, R. Guilard, Inorg. Chem. 24 (1985) 4521–4528.
[26] K.M. Kadish, D. Sazou, Y.M. Liu, A. Saoiabi, M. Ferhat, R. Guilard, Inorg. Chem. 27 (1988) 1198–1204.
[27] M. Gouterman, in: D. Dolphin (Ed.), The Porphyrins, vol. 1, Academic Press, New York, 1978, pp. 100–109.
[28] H. Brand, J. Arnold, Angew. Chem. Int. Ed. Engl. 33 (1994) 95–97.
[29] C.J. Chang, Y. Deng, A.F. Heyduk, C.K. Chang, D.G. Nocera, Inorg. Chem. 39 (2000) 959–966.
[30] C.J. Chang, E.A. Baker, B.J. Pistorio, Y. Deng, Z.H. Loh, S.E. Miller, S.D. Carpenter, D.G. Nocera, Inorg. Chem. 41 (2002) 3102–3109.
[31] C.J. Chang, Y. Deng, S.M. Peng, G.H. Lee, C.Y. Yeh, D.G. Nocera, Inorg. Chem. 41 (2002) 3008–3016.
[32] L.L. Chng, C.J. Chang, D.G. Nocera, J. Org. Chem. 68 (2003) 4075–4078.
[33] B.J. Pistorio, C.J. Chang, D.G. Nocera, J. Am. Chem. Soc. 124 (2002) 7884–7885.